

# Unsupervised Graph-based Rank Aggregation for Improved Retrieval

Icaro Cavalcante Dourado<sup>a,\*</sup>, Daniel Carlos Guimarães Pedronette<sup>b</sup>, Ricardo da Silva Torres<sup>a</sup>

<sup>a</sup>*Institute of Computing, University of Campinas (UNICAMP), Campinas, Brazil*

<sup>b</sup>*Department of Statistics, Applied Mathematics and Computing, São Paulo State University (UNESP), Rio Claro, Brazil*

---

## Abstract

This paper presents a robust and comprehensive graph-based rank aggregation approach, used to combine results of isolated ranker models in retrieval tasks. The method follows an unsupervised scheme, which is independent of how the isolated ranks are formulated. Our approach is able to combine arbitrary models, defined in terms of different ranking criteria, such as those based on textual, image or hybrid content representations.

We reformulate the ad-hoc retrieval problem as a document retrieval of their fusion graph, which we propose as a new unified representation model capable of merging multiple ranks and expressing inter-relationships of retrieval results automatically. By doing so, we claim that the retrieval system can benefit from learning the manifold structure of datasets, thus leading to more effective results. Another contribution is that our graph-based aggregation formulation, unlike existing approaches, allows for encapsulating contextual information encoded from multiple ranks, which can be directly used for ranking, without further computations and processing steps over the graphs. Based on the graphs, a novel similarity retrieval score is formulated using an efficient computation of minimum common subgraphs. Finally, another benefit over existing approaches

---

\*Corresponding author.

*Email addresses:* `icaro.dourado@ic.unicamp.br` (Icaro Cavalcante Dourado), `daniel@rc.unesp.br` (Daniel Carlos Guimarães Pedronette), `rtorres@ic.unicamp.br` (Ricardo da Silva Torres)

is the absence of hyperparameters.

A comprehensive experimental evaluation was conducted considering diverse well-known public datasets, composed of textual, image, and multimodal documents. Performed experiments demonstrate that our method reaches top performance, yielding better effectiveness scores than state-of-the-art baseline methods and promoting large gains over the rankers being fused, thus showing the successful capability of the proposal in representing queries based on a unified graph-based model of rank fusions.

*Keywords:* rank aggregation, content-based retrieval, graph-based fusion

---

## 1. Introduction

The increasing demand of effective and efficient retrieval methods, due to the huge growth of the volume and diversity of available data, has encouraged the creation of sophisticated feature extraction algorithms. These algorithms are important due to being the basis of subsequent generalization and learning models, such as for retrieval or classification tasks. The proposal of description approaches for images, texts, and multimedia data has advanced in the last decades, leading to more discriminative and precise models. However, the choice of the most suitable technique often depends on the circumstances (e.g., application or dataset) in which they are used. In fact, an active research venue relies on exploiting their complementary view, by aggregation, aiming to improve the effectiveness of complex services, such as search and recommendation.

Rank aggregation techniques are important in many applications, such as meta-search, document filtering, recommendation systems, social choice, etc. Unsupervised and supervised rank aggregation methods have been proposed in order to combine results from different rankers and promote more effective retrieval results. Although supervised methods have the potential to produce better fusions, in practice they demand more computational cost, and require training data that may be either unavailable or expensive to obtain. A crowd paradigm, aimed at obtaining labeled training data through voluntary or paid

collaborative work, can mitigate the lack of training data, but this can still be a time-consuming, expensive, unfeasible process or introduce bias to data.

Several different strategies have been exploited by rank aggregation methods, mainly based on available information provided by retrieval scores (Fox and Shaw, 1994) or positions in ranks (Borda, 1784; Cormack et al., 2009). Another common approach is based on Markov Chain, where retrieved objects are represented in the various ranks as vertices in a graph, and transition probabilities from vertex to vertex are defined in terms the relative positions of the items in the various ranks (Sculley, 2007; Dwork et al., 2001). In fact, graphs have been proved to be a powerful tool for modeling the relationships among data objects in recent rank aggregation approaches (Zhang et al., 2015; Pedronette et al., 2017).

In this paper, we propose an unsupervised graph-based rank aggregation method, agnostic of the rankers being fused, and targeted for general applicability, such as image, textual, or even multimodal retrieval tasks. We reformulate the ad-hoc retrieval problem as a document retrieval of their fusion graph, which we propose as a new unified representation model capable of merging multiple ranks and express inter-relationships of retrieval results automatically. By doing so, our main research objective is to investigate our hypothesis that the retrieval system can benefit from learning the manifold structure of datasets, thus promoting more effective results.

As we model and retrieve objects by multiple rankers, the main application of our method is ad-hoc retrieval, also called content-based retrieval, in which images, documents or even multimodal objects are used as queries in a retrieval system. This application can be adopted for digital libraries, social media, service providers, etc. Content-based image retrieval (CBIR), for instance, is an existent field for application.

Another research objective consists in investigating the impact of different ranker selection criteria for fusion, which take into account the rankers' effectiveness and their correlation.

Different from most related rank aggregation approaches, the proposed

method does not require free parameters, such as neighborhood size definition for the graph construction. The proposed method is also innovative with regard to the definition of the fused retrieval score. While other related graph-based approaches exploit the graph through operations on transition matrices (Zhang et al., 2015) or specific similarity measures (Pedronette et al., 2017), our approach derives a new retrieval score directly based on the graph structure, considering the minimum common subgraph of two objects’ graphs. In summary, our fusion method relies on exploiting contextual information obtained from the direct comparison of objects based on their neighbors, which are defined in terms of the ranks associated with multiple ranking criteria.

The contributions of the work are:

1. The proposal of a novel rank aggregation model, that is unsupervised, does not require tuning of hyperparameters, and yields top performance compared to state-of-the-art methods, and large gains over the rankers being fused;
2. The proposal of a unified graph-based representation model that is capable of merging multiple ranks and expressing inter-relationships of retrieval results automatically;
3. The fusion model is agnostic about the ranks, such as how they are generated, their weighting functions, whether distance based or similarity based, etc.;
4. The fusion is multimodal, meaning that it can be applied over different types of data at same time;
5. Unlike existing approaches, a straightforward ranking procedure is proposed, for the fusion representation. The method does not require optimizations or additional processing steps;
6. A novel similarity score is formulated, based on the fusion graphs, using an efficient computation of minimum common subgraphs;
7. The fusion graph extraction and the graph-based retrieval are independent, both being capable of adaptation or further improvement.

The remainder of this paper is organized as follows. Section 2 discusses related work and Section 3 formally describes the retrieval model considered. Section 4 presents the proposed method and Section 5 describes conducted experiments. Finally, Section 6 concludes the paper and provides possible future research directions.

## 2. Related Work

Rank aggregation can be seen as the task of finding a good permutation of retrieved objects obtained from different input ranks. The Kemeny rank aggregation problem consists of finding the optimal permutation. It is an NP-hard problem for more than three input ranks (Dwork et al., 2001). In practice, rank aggregation methods compose inexact solutions that intend to promote better results than the isolated input ranks.

Related to the rank aggregation task, *re-ranking* refers to a prior family of methods that also intend to promote better results, but do not explore the inter-relationships between the ranks from the response objects. Re-ranking approaches are feature-based (Hubert et al., 2018) or the rank-based (Bai and Bai, 2016). In this sense, the exploitation of inter-relationships between ranks is a potential advantage for the rank aggregation methods by definition. Besides, the main advantage of ranked-based approaches for improved retrieval, over feature-based approaches, is that while digital objects are typically modeled in high dimensional spaces, they often live in a much lower-dimensional intrinsic manifold space (Zhao et al., 2018). For this reason, ranked-based approaches can be more efficient while assuming less input data.

Supervised rank aggregation methods are intended to infer fusion formulations automatically from training data, by exploiting labeled information and ground-truth relevance to maximize the effectiveness of a new ranker. Supervised rank aggregation methods belong to the Learning-to-Ranking (L2R) field, which refers to a broader family of supervised methods for ranking. As a drawback, the availability of training data is not always possible or feasible, and

supervised techniques demand more computational cost.

Kaur et al. (2017) proposed a metaheuristic approach, based on genetic algorithm (GA), that optimizes the rank aggregation problem for search engines. The GA approach applies an optimization process over distance measures to minimize the distances for various aggregated ranks to generate a final aggregated rank. Mourão and Magalhães (2018) proposed Learning to Fuse (L2F), a L2R algorithm of presumably lower complexity than other more costly L2R models but with competitive retrieval results to them. It mitigates the final complexity by analyzing and discarding ranks of minor improvements to final rank, during its learning process, thus trading precision for complexity. In our opinion, such supervised rank aggregation models are still either too complex, data-dependent or costly to scenarios in which unsupervised models can be satisfactory. Here we focus on unsupervised methods for rank aggregation.

Rank aggregation methods are also classified as order-based or score-based. Order-based methods use the relative order among the retrieved objects to aggregate the ranks. Score-based methods also use the scores associated with each retrieved object from different ranks as input.

BordaCount (Borda, 1784) is an order-based method that computes a new score of each retrieved object based on the disparity between its positions on the ranks with respect to the their sizes. Reciprocal Rank Fusion (RRF) (Cormack et al., 2009), by contrast, is an order-based method that assigns scores to retrieved objects using a formulation that more emphatically penalizes lower-ranker results in favor of highly ranked results.

Median Rank Aggregation (MRA) (Fagin et al., 2003) is an order-based method. It traverses the ranks counting the number of occurrences of the retrieved objects. The first object that occurs in more than half of the ranks is taken as the first object of the final rank. Then, the second object that occurs in more than half of the ranks is taken as the second, and so on.

Six score-based methods were proposed by Fox and Shaw (1994): CombSUM, CombMAX, CombMIN, CombMED, CombMNZ, and CombANZ, based on distinct priors. For these methods, each rank must be previously normalized

with respect to its scores. Related to these methods, RLSim (Pedronette and Torres, 2013) is a score-based technique, inspired by Naive Bayes classifier, that assigns the final score of an object as the product of its scores in each rank.

Condorcet is a voting method, based on the Condorcet criterion. This criterion defines that the winner of the election is the candidate that beats the other candidates in pairwise comparisons. Let the distance between two ranks be the number of pairs whose objects are ranked reversely. The Condorcet winner is the one that minimizes the total distance. The Condorcet method produces a ranking of all candidates from the first to the last place. The Condorcet winner comes first and the Condorcet loser comes last.

Some graph-based approaches for rank fusion were proposed based on Markov Chains, where retrieved objects are represented in the various ranks as vertices in a graph, with transition probabilities from vertex to vertex defined by the relative rankings of the items in the various ranks (Sculley, 2007; Dwork et al., 2001).

Zhang et al. (2015) proposed a graph-based rank aggregation method, named here as QueryRankFusion, that explores the notion of reciprocal references. It analyzes the  $k$ -reciprocal neighborhoods for building a graph for each rank, and requires the computation of the Jaccard measure for assigning weights to edges. Graphs are later fused into a global graph. Then, it relies on a ranking step using two possible solvers, either based on the PageRank algorithm that computes a transition matrix over the edges or by a greedy algorithm that finds subgraphs of maximum local density. This method depends on the adjustment of three hyperparameters: the number  $k$  of neighbors to analyze; the solver algorithm for the ranking step; and the number of iterations in the ranking step. This method yields effective results, but it was validated only for image retrieval tasks. Equivalently, Pedronette et al. (2016) proposed RkGraph, a graph-based aggregation approach for distance learning in shape retrieval tasks, which merges graphs defined upon multiple ranks and composes a collection graph.

Pedronette and Torres (2016) proposed CorGraph, a learning method based

on a correlation graph, which defines the graph connectivity using different levels of correlation measures and exploits strongly connected components. Pedronette et al. (2017) continued their work proposing a simpler graph-based method, hereby called RecKNNGraphCCs, as in Zhang et al. (2015), but with less intermediate steps and less hyperparameters. In their method, they rely on connected components in the step of generating ranks. A pre-processing step of re-ranking and normalization is performed to improve the ranks before the use of the rank aggregation scheme. This method is affected by two hyperparameters: the number of iterations and the number of neighbors to analyze. This method was also validated only in image retrieval problems.

Existing graph-based methods are mostly targeted at modelling the whole collection of objects as a graph, from which the ranks can be derived. Different from these works, we model one fusion graph per object, and redefine the object retrieval system by means of fusion graphs. Our graph definition not only encapsulates the information from ranks of a certain query, but also incorporates information regarding inter-relationships between the results from the ranks.

Our approach presents theoretical and practical advances and implications. A theoretical implication is that ranks can be directly used for fusion, thus promoting a unified representation. From this representation, called fusion graph, we derive a straightforward ranking procedure, without further transformations and optimizations. That corresponds to the second theoretical implication. A practical implication from our approach is its advantage that the fusion graph extraction and the graph-based retrieval are independent, both being capable of adaptation or further improvement. In addition, as another practical implication, it does not require time-consuming tuning of hyperparameters.

### 3. Retrieval Model

Our approach for ranking is based upon the following definitions. Let  $S = \{s_1, s_2, \dots, s_n\}$  be a collection of  $n$  *samples*, where  $n$  is the collection size. A sample can be a document, an image, a video, or even a hybrid (called mul-



timodal) object. Each sample  $s$  from  $S$  is characterized (or described) by *descriptors*. Each descriptor,  $\mathcal{D}$ , has its own assumption, pros and cons, and represents a specific point of view with respect to the samples. For this reason, it is common to use multiple descriptors to characterize a collection. A descriptor is used to assign (extract from the object) to  $s$ , a vector, a graph, or any data structure  $\epsilon(s)$ . The purpose of  $\epsilon(s)$  is to allow the comparison of objects, supporting the creation of services, such as search or recommendation. Comparisons are performed by means of a *comparator*,  $\mathcal{C}$ , applied over a tuple  $(\epsilon(s_i), \epsilon(s_j))$ , that produces a *score*  $\varsigma$  of codomain  $\mathbb{R}^+$  (e.g., the cosine similarity and the Euclidean distance) in the sense that either similarity or dissimilarity functions can be used. We employ a special procedure to convert dissimilarity into similarity scores, so that different kinds of ranks can be combined. We present our standardization procedure in Section 4.1.1.

A query sample  $q$ , or just *query*, follows the same definition of a sample, but refers to the input object in the context of a search: a search brings *response items* (samples) from the *response set* ( $S$ ) according to a relevance criteria. We refer to a *ranker* as a tuple  $R = (\mathcal{D}, \mathcal{C})$ , which is employed to compute a rank,  $\tau$ , for  $q$ . A ranker may be seen as a *retrieval model*, from the information retrieval literature. We denote by  $\tau_q$  the rank for a certain input query  $q$ . A rank is a permutation of  $S_L \subseteq S$ , where  $L \ll n$  in general, such that  $\tau_q$  provides the most similar – or equivalently the least dissimilar – samples, to  $q$ , from  $S$ , in order.  $L$  is used as a cut-off parameter.  $\rho_{\tau_q}(x)$  refers to the position of  $x$  in  $\tau_q$ .

Given a certain ranker  $R$ , we may refer to  $\varsigma(s_i, s_j)$  as meaning  $\varsigma(\epsilon(s_i), \epsilon(s_j))$ , for simplicity.  $s_i$  occurs closer to the first positions of  $\tau_q$  than  $s_j$  if  $\varsigma(q, s_i) \leq \varsigma(q, s_j)$ . Along with one rank  $\tau_q$  – a sequence of objects  $s_i$  – we also hold the scores  $\varsigma(q, s_i)$  in order to use them in our rank aggregation function, together with proper normalization steps. The notation  $\varsigma_{\tau_q}(s_i, s_j)$  stands for the general case, which is the score between  $s_i$  and  $s_j$  with respect to the same descriptor and comparator from the ranker that produced the rank  $\tau_q$  for the query  $q$ .

While a ranker establishes a ranking model, different descriptors and comparators can be used to compose rankers, and it is well known that descrip-

tors can be complementary, as well as comparators. Given a set of  $m$  rankers,  $\{R_1, R_2, \dots, R_m\}$ , being used for query retrieval over a collection  $S$ , for every query  $q$  we can obtain  $\mathcal{T}_q = \{\tau_1, \tau_2, \dots, \tau_m\}$ , from which a *rank aggregation* function  $f$  can produce a combined rank  $\tau_{q,f} = f(\mathcal{T}_q)$ , hopefully more effective than the individual ranks  $\tau_1, \tau_2$ , etc.

We summarize the notations and their definitions in Table 1.

Table 1: Notations followed in our Retrieval Model.

Notation	Meaning
$S$	collection, or the response set in the context of search
$n$	$ S $
$s$	a sample, from $S$
$\mathcal{D}$	descriptor
$\epsilon(s)$	a data structure, generated by $\mathcal{D}$ , that describes $s$
$\mathcal{C}$	comparator
$\varsigma$	score, of codomain $\mathbb{R}^+$ , generated by $\mathcal{C}$ over $(\epsilon(s_i), \epsilon(s_j))$
$q$	query
$L$	cut-off parameter
$R$	ranker, a tuple $(\mathcal{D}, \mathcal{C})$
$\tau$	rank, a permutation of $S_L \subseteq S$ , generated by $R$
$\tau_q$	rank for $q$
$\varsigma_{\tau_q}(s_i, s_j)$	score between $s_i$ and $s_j$ with respect to the same $R$ that produced $\tau_q$ for $q$
$\rho_{\tau_q}(x)$	position of $x$ in $\tau_q$
$m$	number of rankers used
$\mathcal{T}_q$	rank set for $q$ , $\{\tau_1, \tau_2, \dots, \tau_m\}$ , generated by $\{R_1, R_2, \dots, R_m\}$
$f$	a rank aggregation function
$\tau_{q,f}$	the output rank of $f$ , expressed by $f(\mathcal{T}_q)$

#### 4. Unsupervised Graph-based Rank Aggregation Approach

We propose a graph-based rank aggregation function  $f$  that works for any collection  $S$  combined with the use of  $m$  rankers of any kind. It relies on a *composite* ranker, whose descriptor extracts a graph-based representation,

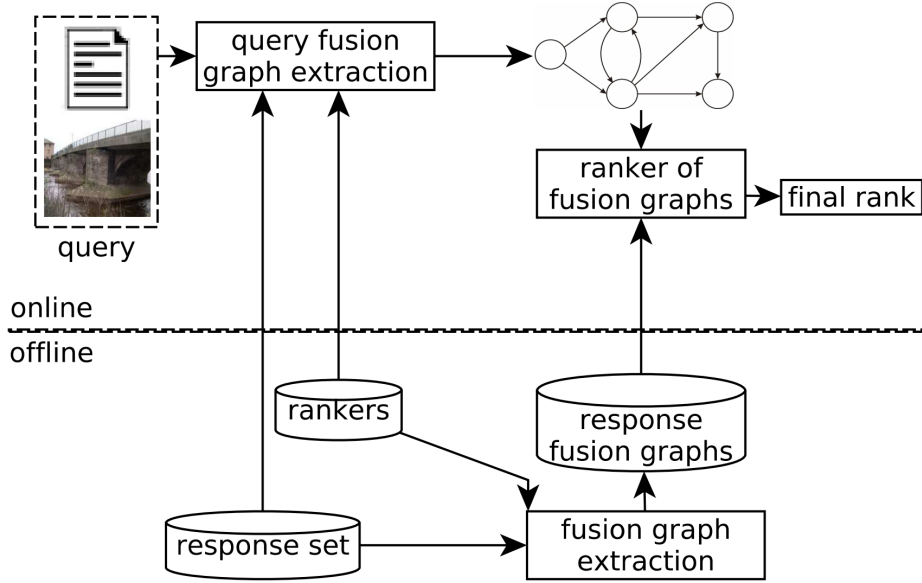


Figure 1: Schematic view of the unsupervised graph-based rank aggregation approach.

named *fusion graph*, from collection samples, and a fusion graph comparator is employed in this ranker. A fusion graph encodes contextual information from different ranks, defined in terms of multiple base rankers.

Both a query  $q$  and each sample  $s$  of a target collection are represented by graphs, say query fusion graph  $G_{\mathcal{T}_q}$  and fusion graph  $G_{\mathcal{T}_s}$ . A search is, therefore, modeled as the ranking of graphs  $G_{\mathcal{T}_s}$  of collection samples with respect to a query graph  $G_{\mathcal{T}_q}$ , i.e., the rank aggregation function  $f$  is able to rank fusion graphs based on their similarity to a query graph.

Figure 1 provides a schematic overview of the unsupervised graph-based rank aggregation approach, which is composed of offline and online workflows. The steps ‘fusion graph extraction’ and ‘ranker of fusion graphs’ are detailed in Sections 4.1 and 4.2, respectively. The offline workflow is responsible for representing the response set as fusion graphs, while the online workflow, in turn, processes a query and produces a final rank to be returned as the final result.

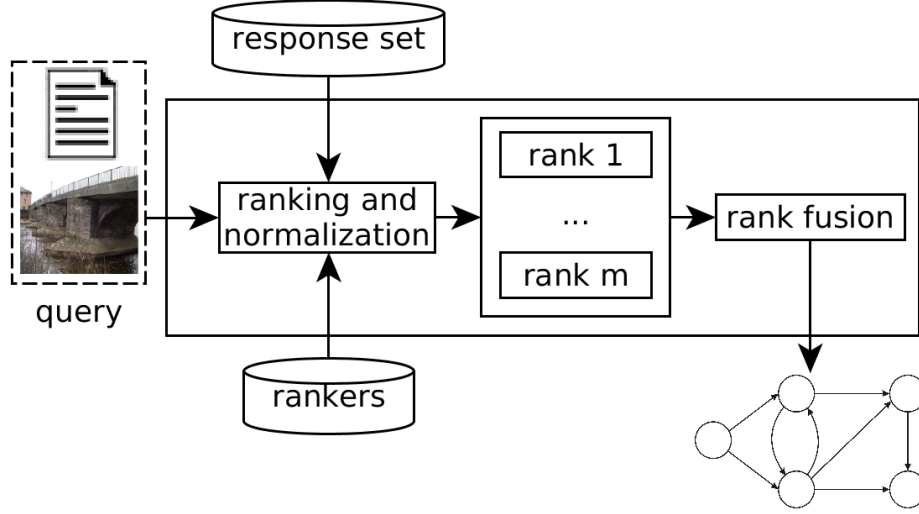


Figure 2: Extraction of a fusion graph.

#### 4.1. Extraction of Fusion Graphs

In both offline and online workflows, illustrated in Figure 1, a fusion graph extraction step is adopted. A fusion graph extraction aggregates ranks for a query, based on the rankers and response set used, producing a fusion graph per query. It is basically comprised of three steps: creation of ranks using different rankers, rank normalization, and rank fusion. These components are illustrated in Figure 2. The creation of ranks follows what was described in Section 3. Our rank aggregation function works upon a predefined set of rankers, so we assume that the base ranks for any query can be provided as requested. Sections 4.1.1 and 4.1.2 detail the other steps.

##### 4.1.1. Rank Normalization

For a certain ranker, its comparator  $\mathcal{C}$  may be either a distance or similarity function. Furthermore, different comparators may produce scores at different ranges. Nevertheless, these scores are employed in our rank aggregation function. For this reason, we need to normalize the comparator outputs, from the rankers being used, so that the scores from ranks become comparable. The

ranks' scores must also fit into an uniform positive range, due to the way we use the scores in our rank aggregation formulation.

Assuming ranks of size  $L$ , we adopt a rank normalization procedure that relies on two steps: rank repositioning based on mutual and reciprocal rank references, and score rescaling.

Rank relationships are not symmetric, in the sense that an object  $i$  well ranked for a query  $j$  does not imply that  $j$  is well ranked for a query  $i$ . However, improving the symmetry of the  $k$ -neighborhood usually improves the effectiveness of retrieval functions (Jegou et al., 2010). In order to explore this behavior, we propose a rank repositioning, based on a neighborhood-aware distance  $\delta$  given by Equation 1, where  $\rho_{\tau_i}(j) \leq L$  and refers to the position of  $j$  in the rank  $\tau_i$ . It considers both mutual (Pedronette and Torres, 2013) and reciprocal (Qin et al., 2011) neighborhood, and the ranks are then updated by a stable sorting algorithm over  $\delta$ , up to the top- $L$  positions. The idea is to bring a ranked item  $i$  to the top positions of the rank of  $j$  as much as  $j$  also has  $i$  in top positions of its own rank. The mutual neighborhood sums rank positions from both ranks, and the reciprocal neighborhood considers only the maximum.

$$\delta(i, j) = \rho_{\tau_i}(j) + \rho_{\tau_j}(i) + \max(\rho_{\tau_i}(j), \rho_{\tau_j}(i)) \quad (1)$$

For the second rank normalization step, we perform score rescaling for the rank, assigning a uniform range from 1, to the top-ranked response item, to 0.1, to the top- $L$  ranked response item, adopting uniform steps within this interval.

#### 4.1.2. Rank Fusion

This step is responsible for producing graphs that reflect the ranks for query samples. At first, in an offline stage, for each sample  $s \in S$ , we perform a search using  $s$  as  $q$  and obtain its corresponding set  $\mathcal{T}_q$  of ranks, using a cut-off of  $L$ .

The choice of  $L$  depends on the intended result size. Due to the way we construct the fusion graph, especially the vertex and edge weights, the value of  $L$  does not directly affect the quality of the model, not demanding empirical adjustment. The effect of changing the value of  $L$  is to increase the effectiveness

of the method, up to a certain limit. In practice, the choice of  $L$  is guided only by the trade-off between efficiency and effectiveness. Our method has only this parameter, as opposed to some related works (Zhang et al., 2015; Pedronette et al., 2017), usually dependent on multiple hyperparameters.

From  $\mathcal{T}$ , we derive a weighted directed graph  $G_{\mathcal{T}} = (V_{\mathcal{T}}, E_{\mathcal{T}})$  that combines information from the ranks of  $\mathcal{T}$ , where  $V_{\mathcal{T}}$  is the vertex set and  $E_{\mathcal{T}}$  is the edge set. A fusion graph aims to be a discriminative and comparable representation of an object, relative to its ranks, and how these ranks relate. In this sense, a fusion graph  $G_{\mathcal{T}_q}$  of an object  $q$  includes all response items from each rank  $\tau_q \in \mathcal{T}_q$ , as vertices, and then relates these vertices, with edges, according to the degree of relationship between them, and between them to  $q$ .

Algorithm 1 illustrates how  $G_{\mathcal{T}}$  is computed. A vertex  $v_A$  is associated with a collection sample  $A$ . The vertex set is composed of the union of all samples found in all ranks defined for query  $q$ . The weight of vertex  $v_A$ ,  $w_{v_A}$ , is the sum of the similarities that the response item  $A$  has in the ranks of  $q$  (lines 5 to 10, Equation 2). The vertex weight is adopted to reflect how relevant a response item  $A$  is to  $q$ .

Edges are created to express the relationship between response items (lines 11 to 20). There will be an edge  $e_{A,B}$ , linking  $v_A$  to  $v_B$ , if  $A$  and  $B$  are both responses in any rank of  $q$  and if  $B$  occurs in any rank of  $A$ . The weight of  $e_{A,B}$ ,  $w_{e_{A,B}}$ , is the sum of the similarities that the response item  $B$  has in the ranks of  $A$ , divided by the position of  $A$  in each rank of  $q$  (Equation 3), considering position values starting by 1. The scores of  $B$  in each  $\tau_A$  matters, so we sum its scores, but we also weight these scores inversely by the position in which  $A$  appears in  $\tau_q$ , for this relationship between  $A$  and  $B$  to take into account the importance with respect to  $q$ .

$$w_{v_A} = \sum_{A \in \tau_i \wedge \tau_i \in \mathcal{T}_q} \varsigma_{\tau_i}(q, A) \quad (2)$$

$$w_{e_{A,B}} = \sum_{A \in \tau_i \wedge \tau_i \in \mathcal{T}_q} \sum_{B \in \tau_j \wedge \tau_j \in \mathcal{T}_A} (\varsigma_{\tau_j}(A, B) \div \rho_{\tau_i}(A)) \quad (3)$$

Algorithm 1: Rank fusion.

```

1 # inputs: ranks  $\mathcal{T}_q$ , for the query  $q$ 
2 # output: a weighted directed graph  $G_{\mathcal{T}}$ 
3  $G_{\mathcal{T}} = \text{WeightedDirectedGraph}() \# (V_{\mathcal{T}}, E_{\mathcal{T}})$ 
4 for  $\tau$  in  $\mathcal{T}_q$ : # create vertices
5     for  $A$  in  $\tau$ :
6         weight =  $\varsigma_{\tau}(q, A)$ 
7         if  $v_A \notin V_{\mathcal{T}}$ : # if new vertex
8              $V_{\mathcal{T}} = V_{\mathcal{T}} \cup v_A$ 
9              $w_{v_A} = \text{weight}$ 
10        else:  $w_{v_A} += \text{weight}$ 
11 for  $\tau$  in  $\mathcal{T}_q$ : # create edges
12     for  $A$  in  $\tau$ :
13         for  $\tau_A$  in  $\mathcal{T}_A$ :
14             for  $B$  in  $\tau_A$ :
15                 if  $v_B \in V_{\mathcal{T}}$  and  $A \neq B$ :
16                     weight =  $\varsigma_{\tau_A}(A, B) \div \rho_{\tau}(A)$ 
17                     if  $e_{A,B} \notin E_{\mathcal{T}}$ : # if new edge
18                          $E_{\mathcal{T}} = E_{\mathcal{T}} \cup e_{A,B}$ 
19                          $w_{e_{A,B}} = \text{weight}$ 
20                     else:  $w_{e_{A,B}} += \text{weight}$ 
21 g.normalizeWeights(0,1)

```

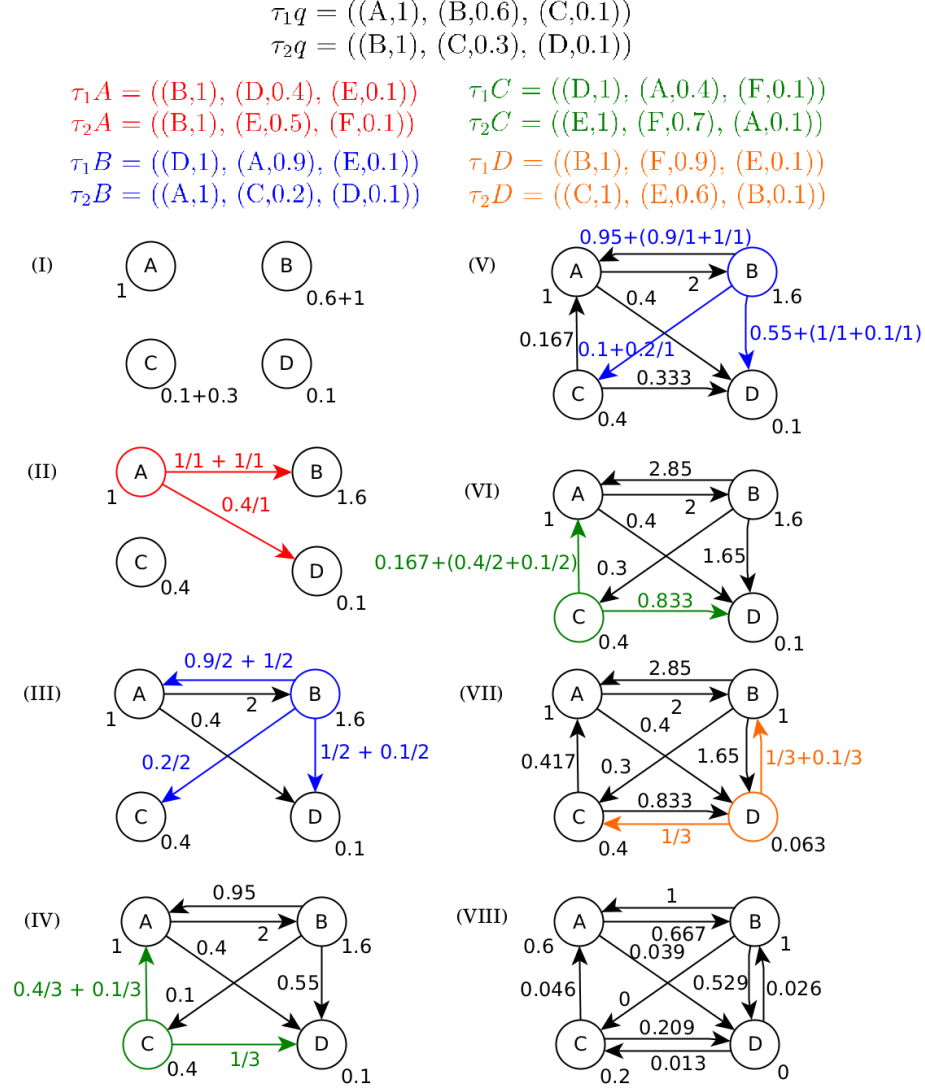


Figure 3: Example of graph construction during rank fusion. The scores are shown along with the response items, within the ranks, for simplicity.

The creation of  $G_{\mathcal{T}}$  ends with a weight normalization (line 21), which makes the graph comparable by means of a graph comparator. The weight of each vertex  $v_i$ ,  $w_{v_i}$ , is replaced by  $\frac{w_{v_i}}{\max(w_v)}$ , and the weight of edge  $e_{i,j}$ ,  $w_{e_{i,j}}$ , is replaced by  $\frac{w_{e_{i,j}}}{\max(w_e)}$ .



Figure 3 illustrates an example for the rank fusion, assuming a query  $q$  and the use of two rankers. At first, a fully disconnected graph is built based on the retrieved results and their scores (I). Then, the relationships between the results (encoded in the ranks for B in blue, C in green, and D in orange), in their own ranks, are propagated into the graph as edges (see III, IV, and V). The resulting graphs, VI and VII in Figure 3, correspond to the final fusion graph before and after normalization, respectively.

#### 4.2. Retrieval based on Fusion Graphs

Our proposed rank aggregation function  $f$  relies on a *composite* ranker that is defined as  $R_G = (D_G, \mathcal{C}_G)$ , where  $D_G$  is a descriptor which extracts fusion graphs, and  $\mathcal{C}_G$  is a fusion graph comparator. Given two fusion graphs  $G_a$  and  $G_b$ ,  $\varsigma(G_a, G_b)$  can be computed by  $\mathcal{C}_G$  using any graph-based similarity or dissimilarity function. We propose the adoption of formulations based on the minimum common subgraph (*mcs*), such as MCS (Bunke and Shearer, 1998) or WGU (Wallis et al., 2001). A graph  $M$  is the *mcs* of two weighted graphs  $G_a$  and  $G_b$  if: (1)  $M \subseteq G_a$  (2)  $M \subseteq G_b$  and (3) there is no other subgraph  $M'$  ( $M' \subseteq G_a$ ,  $M' \subseteq G_b$ ), such that  $|M'| > |M|$ , where  $|M|$  is given by the sum of the vertex weights and edge weights of  $M$ .

MCS and WGU are shown in Equation 4 and 5, respectively. In MCS, the larger the  $|mcs|$  is, the more similar the two graphs are, which decreases the distance up to 0. This metric produces values in  $[0, 1]$ . WGU behaves similarly to MCS with respect to identical graphs or graphs without intersection, and also produces values in  $[0, 1]$ . The denominator in WGU represents the size of the union of the two graphs, whose motivation is to allow for changes in the smaller graph to influence the distance value, which is not covered in MCS. In a preliminary analysis, for our graph formulation WGU performed better in all cases, so we ended up choosing it.

$$dist_{MCS(G_a, G_b)} = 1 - \frac{|mcs(G_a, G_b)|}{\max(|G_a|, |G_b|)} \quad (4)$$

$$dist_{WGU}(G_a, G_b) = 1 - \frac{|mcs(G_a, G_b)|}{|G_a| + |G_b| - |mcs(G_a, G_b)|} \quad (5)$$

Note that the scores  $\varsigma(G_{\mathcal{T}_q}, G_{\mathcal{T}_{s_i}})$  and  $\varsigma(G_{\mathcal{T}_q}, G_{\mathcal{T}_{s_j}})$  can be compared to infer whether  $s_i$  or  $s_j$  is more relevant to  $q$ . The higher the score, the most similar the query and the response item are, regarding their ranks. A fusion graph, therefore, is able to encode intrinsic contextual information from multiple ranks.

The rank aggregation function  $f$  is defined as  $f(\mathcal{T}_q) = \tau_{q,f} = \{s_1, s_2, \dots, s_n\}$  such that  $|\tau_{q,f}| \leq L$  and  $\{\varsigma(G_{\mathcal{T}_q}, G_{\mathcal{T}_{s_1}}), \varsigma(G_{\mathcal{T}_q}, G_{\mathcal{T}_{s_2}}), \dots, \varsigma(G_{\mathcal{T}_q}, G_{\mathcal{T}_{s_n}})\}$  is in increasing order.

#### 4.3. Computational Cost Analysis

The cost of executing a query  $q$  is the sum of the costs for: generating the ranks  $\mathcal{T}_q$  for  $q$ ; generating the query fusion graph  $G_{\mathcal{T}_q}$ ; and retrieving samples using  $G_{\mathcal{T}_q}$  and response set fusion graphs.

For the first part, individual ranks  $\tau \in \mathcal{T}_q$  can be generated in parallel. Therefore, this step is limited by the cost of the slowest ranker. Note that, typically, rankers adopt indexing structures, such as KD-tree or inverted files, leading to rank generations in sub-linear time with respect to the response set.

For the second part, the Rank fusion (Algorithm 1) has an asymptotic cost of  $O(mL)$  for the first outer loop (create vertices), and  $O(mLmL)$  for the second outer loop (create edges), leading to a total cost of  $O(m^2L^2)$ . As we use small values of  $L$  and also a small number ( $m$ ) of rankers, the cost of the rank fusion algorithm itself is negligible when compared to the step concerned with the generation of ranks.

In our fusion graph, vertices have different labels, and therefore we use graph comparison functions that take advantage of efficient algorithms for computing minimum common subgraphs, reducing its asymptotic cost to  $O(|V_1||V_2|)$  (Dickinson et al., 2004). Note also that the number of vertices in each graph is  $O(mL)$  in the worst case. Both aspects lead to efficient graph comparators, in practice. The graph-based retrieval can be either implemented linearly over the response set, or sub-linearly using indexing methods such as graph embedding

Table 2: Datasets used in the experimental evaluation.

Dataset	Size	Type
Ohsumed	34,389	Textual
Brodatz	1,776	Texture
MPEG-7	1,400	Shape
Soccer	280	Color Scenes
UW	1,109	Color Scenes and Keywords
UKBench	10,200	Objects / Scenes

techniques (Silva et al., 2018; Zhu et al., 2014). We leave this investigation for future work.

The graph-based retrieval, for each  $q$ , relies on the existence of ranks and fusion graphs from the response set, but both steps are performed only once per collection (‘fusion graph extraction’ in Figure 1), and in an offline stage.

## 5. Experimental Evaluation

This section presents the adopted evaluation protocol and experimental results related to the comparison of our method with individual rankers and other rank aggregation approaches.

### 5.1. Datasets and features

We selected datasets of different purposes, compositions, and sizes in order to validate our method in different searching scenarios. Table 2 lists the datasets used, and Table 3 summarizes the individual rankers being adopted per dataset in order to (1) be evaluated in isolation, and (2) generate rankers for the fusions.

**Ohsumed** (Hersh et al., 1994) is a textual dataset, composed of bibliographic medical documents, provided by the National Library of Medicine. It contains 34,389 cardiovascular diseases abstracts, distributed across 23 Medical Subject Headings (MeSH) diseases categories of cardiovascular diseases group. Without loss of generality, we used the subset of 18,302 uni-labeled documents,

Table 3: Individual rankers adopted per dataset in the experimental evaluation.

Dataset	Rankers	Type
Ohsumed	BoW-cosine, BoW-Jaccard, 2grams-cosine, 2grams-Jaccard, GNF-MCS, GNF-WGU, WMD	Textual
Brodatz	LBP, CCOM, LAS	Texture
MPEG-7	SS, BAS, IDSC, CFD, ASC, AIR	Shape
Soccer	GCH, ACC, BIC	Color
UW	GCH, BIC, JAC, HTD, QCCH, LAS, CO-SINE, JACCARD, TF-IDF, DICE, OKAPI, BOW	Color, Texture, Textual
UKBench	ACC, VOC, SCD, JCD, CNN-Caffe, FCTH-SPy, CEDD-SPy	Color, Texture, BoVW, CNN

varying from 56 to 2876 documents per category. For Ohsumed, we adopted 7 rankers<sup>1</sup>:

- 2 using the Bag-of-Words (BoW), with comparators cosine and Jaccard: BoW-cosine and BoW-Jaccard;
- 2 using the 2grams descriptor, with comparators cosine and Jaccard: 2grams-cosine and 2grams-Jaccard;
- 2 using a graph-based descriptor, called *normalized-frequency* (GNF) (Schenker et al., 2007), with comparators MCS (Bunke and Shearer, 1998) and WGU (Wallis et al., 2001): GNF-MCS and GNF-WGU;
- WMD (Kusner et al., 2015), a ranker based on *word embeddings* (Mikolov et al., 2013).

<sup>1</sup>For all textual rankers used in the experimental evaluation, we preprocess the documents with stop word removal and Porter’s stemming.

**Brodatz** (Brodatz, 1966) is a texture dataset. There are 1,776 images (texture blocks), being 16 samples for each of the 111 classes (texture types). We adopt 3 texture rankers: Local Binary Patterns (LBP) (Ojala et al., 2002), Color Co-Occurrence Matrix (CCOM) (Kovalev and Volmer, 1998), and Local Activity Spectrum (LAS) (Tao and Dickinson, 2000).

**MPEG-7** (Latecki et al., 2000) is a shape dataset, composed of 1400 images, equally distributed in 20 images per 70 categories. We adopt 6 shape rankers: Segment Saliences (SS) (Torres and Falcão, 2007), Beam Angle Statistics (BAS) (Arica and Vural, 2003), Inner Distance Shape Context (IDSC) (Ling and Jacobs, 2007), Contour Features Descriptor (CFD) (Pedronette and Torres, 2010), Aspect Shape Context (ASC) (Ling et al., 2010), and Articulation-Invariant Representation (AIR) (Gopalan et al., 2010).

**Soccer** (Van De Weijer and Schmid, 2006) is an image dataset, composed of 280 images, equally distributed in 40 images per 7 categories (the soccer teams). We adopt 3 color-based rankers: Global Color Histogram (GCH) (Swain and Ballard, 1991), Auto Color Correlograms (ACC) (Huang et al., 1997), and Border/Interior Pixel Classification (BIC) (Stehling et al., 2002).

University of Washington (**UW**) (Deselaers et al., 2008) is a hybrid dataset, composed of 1109 pictures from different locations, annotated by textual keywords. The number of keywords per picture vary from 1 to 22. There are 20 classes, varying from 22 to 255 pictures per class. We adopt 12 rankers, comprising 3 types:

- 3 Visual color rankers: GCH (Swain and Ballard, 1991), BIC (Stehling et al., 2002), and Joint Autocorrelogram (JAC) (Williams and Yoon, 2007);
- 3 Visual texture rankers: Homogeneous Texture Descriptor (HTD) (Wu et al., 1999), Quantized Compound Change Histogram (QCCH) (Huang and Liu, 2007), and Local Activity Spectrum (LAS) (Tao and Dickinson, 2000);
- 6 Textual rankers: COSINE (Baeza-Yates and Ribeiro-Neto, 1999), JAC-

CARD (Lewis et al., 2006), Term Frequency-Inverse Document Frequency (TF-IDF) (Baeza-Yates and Ribeiro-Neto, 1999), DICE (Lewis et al., 2006), OKAPI (Robertson et al., 1994), and BOW (Carrillo et al., 2009).

**UKBench** (Nistér and Stewénus, 2006) is a dataset of 10,200 images, consisting of 2,550 scenes/objects captured 4 times each. The captures vary in terms of viewpoint, illumination, and distance. The objects/scenes correspond to the categories, so there are four samples per class. Due to the small and fixed category sizes, effectiveness assessment using this dataset relies on an evaluation metric, called N-S Score, varying from 1 to 4, which measures the mean number of relevant images among the first four images retrieved. We adopt seven rankers, based on color and texture properties. Some of them are based on global descriptors, while others rely on local features:

- ACC (Huang et al., 1997);
- Vocabulary Tree (VOC) (Wang et al., 2011), that uses SIFT;
- CNN-Caffe (Jia et al., 2014): features extracted from the 7th layer of a Convolution Neural Network (CNN) obtained with the Caffe framework. A 4096-dimensional descriptor is extracted per image, and the Euclidean distance is used as the comparator.
- Scalable Color Descriptor (SCD) (Manjunath et al., 2001)
- Joint Composite Descriptor (JCD) (Zagoris et al., 2010)
- Fuzzy Color and Texture Histogram Spatial Pyramid (FCTH-SPy) (Chatzichristofis and Boutalis, 2008b; Lux, 2011)
- Color and Edge Directivity Descriptor Spatial Pyramid (CEDD-SPy) (Chatzichristofis and Boutalis, 2008a; Lux, 2011)

## 5.2. Experimental Procedure

We evaluate our method, as well as the individual rankers and baselines, with respect to the effectiveness in retrieval tasks.

Table 4: Results for individual rankers on textual, image, and hybrid datasets.

(a) Brodatz		(c) MPEG-7		(e) UKBench	
Ranker	NDCG@10	Ranker	NDCG@10	Ranker	N-S Score
LAS	0.850533	ASC	0.941585	VOC	3.54
CCOM	0.726186	AIR	0.939424	ACC	3.37
LBP	0.652759	CFD	0.930685	CNN-Caffe	3.31
(b) UW dataset		IDSC	0.922828	SCD	3.15
Ranker	NDCG@10	BAS	0.866098	JCD	2.79
JAC	0.810729	SS	0.611481	FCTH-SPy	2.73
BIC	0.746454			CEDD-SPy	2.61
DICE	0.722831	(d) Ohsumed		(f) Soccer	
BOW	0.720781	Ranker	NDCG@10	Ranker	NDCG@10
OKAPI	0.716035	BoW-cosine	0.669701	BIC	0.614818
JACCARD	0.701651	2grams-cosine	0.664120	ACC	0.592699
TF-IDF	0.658880	GNF-WGU	0.662668	GCH	0.536412
GCH	0.630315	GNF-MCS	0.655420		
COSINE	0.554767	2grams-Jaccard	0.651320		
LAS	0.514314	BoW-Jaccard	0.645711		
HTD	0.495002	WMD	0.427361		
QCCH	0.414249				

Table 5: Correlation of individual ranks on Brodatz.

	CCOM	LAS	LBP
CCOM	1.00	0.38	0.25
LAS	0.38	1.00	0.30
LBP	0.25	0.30	1.00

Table 6: Correlation of individual ranks on UW.

	BIC	GCH	HTD	JAC	LAS	QCCH	BOW	COSINE	DICE	JACCARD	OKAPI	TF-IDF
BIC	1.00	0.29	0.12	0.27	0.12	0.11	0.14	0.11	0.14	0.13	0.13	0.11
GCH	0.29	1.00	0.11	0.18	0.11	0.10	0.11	0.08	0.11	0.10	0.09	0.08
HTD	0.12	0.11	1.00	0.12	0.12	0.12	0.09	0.07	0.09	0.08	0.07	0.07
JAC	0.27	0.18	0.12	1.00	0.11	0.10	0.14	0.11	0.15	0.14	0.13	0.12
LAS	0.12	0.11	0.12	0.11	1.00	0.16	0.08	0.06	0.08	0.08	0.07	0.07
QCCH	0.11	0.10	0.12	0.10	0.16	1.00	0.08	0.06	0.08	0.07	0.06	0.06
BOW	0.14	0.11	0.09	0.14	0.08	0.08	1.00	0.22	0.44	0.42	0.30	0.25
COSINE	0.11	0.08	0.07	0.11	0.06	0.06	0.22	1.00	0.32	0.32	0.36	0.45
DICE	0.14	0.11	0.09	0.15	0.08	0.08	0.44	0.32	1.00	0.85	0.37	0.37
JACCARD	0.13	0.10	0.08	0.14	0.08	0.07	0.42	0.32	0.85	1.00	0.38	0.37
OKAPI	0.13	0.09	0.07	0.13	0.07	0.06	0.30	0.36	0.37	0.38	1.00	0.60
TF-IDF	0.11	0.08	0.07	0.12	0.07	0.06	0.25	0.45	0.37	0.37	0.60	1.00

Table 7: Correlation of individual ranks on MPEG-7.

	AIR	ASC	BAS	CFD	IDSC	SS
AIR	1.00	0.31	0.27	0.30	0.30	0.18
ASC	0.31	1.00	0.33	0.37	0.70	0.20
BAS	0.27	0.33	1.00	0.48	0.32	0.28
CFD	0.30	0.37	0.48	1.00	0.36	0.26
IDSC	0.30	0.70	0.32	0.36	1.00	0.19
SS	0.18	0.20	0.28	0.26	0.19	1.00

Table 8: Correlation of individual ranks on Ohsumed.

	BoW-cosine	BoW-Jaccard	2grams-cosine	2grams-Jaccard	GNF-MCS	GNF-WGU	WMD
BoW-cosine	1.00	0.56	0.48	0.45	0.49	0.55	0.10
BoW-Jaccard	0.56	1.00	0.41	0.50	0.51	0.54	0.11
2grams-cosine	0.48	0.41	1.00	0.64	0.51	0.58	0.10
2grams-Jaccard	0.45	0.50	0.64	1.00	0.55	0.61	0.10
GNF-MCS	0.49	0.51	0.51	0.55	1.00	0.73	0.10
GNF-WGU	0.55	0.54	0.58	0.61	0.73	1.00	0.10
WMD	0.10	0.11	0.10	0.10	0.10	0.10	1.00



Table 9: Correlation of individual ranks on UKBench.

	ACC	VOC	CNN-Caffe	SCD	JCD	FCTH-SPy	CEDD-SPy
ACC	1.00	0.23	0.22	0.31	0.23	0.22	0.21
VOC	0.23	1.00	0.24	0.22	0.21	0.20	0.20
CNN-Caffe	0.22	0.24	1.00	0.21	0.20	0.19	0.19
SCD	0.31	0.22	0.21	1.00	0.26	0.26	0.23
JCD	0.23	0.21	0.20	0.26	1.00	0.39	0.53
FCTH-SPy	0.22	0.20	0.19	0.26	0.39	1.00	0.28
CEDD-SPy	0.21	0.20	0.19	0.23	0.53	0.28	1.00

Table 10: Correlation of individual ranks on Soccer.

	BIC	ACC	GCH
BIC	1.00	0.46	0.27
ACC	0.46	1.00	0.30
GCH	0.27	0.30	1.00

Due to the nature of the datasets used, we use each sample  $s$  as query  $q$  at a time, whose result candidates belong to  $S$ , and we consider a retrieved item as relevant to the query if it belongs to the same class of the query sample, since we are validating in labeled collections, i.e., relevant labels in the experiments are either 1 for relevant or 0 for irrelevant. Therefore, in this case, the query set size corresponds to the dataset size. Separate query and response sets can be used, as well as graded relevance, but these aspects do not affect the applicability of our model. This protocol concerns document retrieval, also referred to as ad hoc retrieval, which was also very usual in validation protocol of our baselines.

We use normalized discounted cumulative gain at cutoff 10 (NDCG@10) for all datasets except UKBench, for which we use the N-S Score, the standard measure used in this dataset.

We adopt  $L = 10$  as a rank cutoff, because we report results for ranks up to sizes 10 for all datasets except UKBench, which uses 4 due to the N-S Score. In fact, this parameter presented very little impact on the re-

sults. Preliminary analysis of effectiveness with respect to  $L$ , varying it in  $\{2, 4, 6, 8, 10, 12, 14, 16, 20\}$ , showed that the effectiveness increased by  $L$  from 2 to 10, and from that point on, the effectiveness measure stabilizes.

For each dataset, we evaluate the effectiveness of the individual rankers<sup>2</sup>, and also their correlation. Both the effectiveness and the correlation scores are used to guide the choice of base rankers. We evaluate three approaches for selecting rankers: all rankers available for each dataset; the pair composed of the two best rankers in terms of effectiveness; and the pair of rankers that present the best balance between high effectiveness and low correlation.

The second and third approaches may lead to the use of the same pair of rankers. Therefore, in cases where this happens, we also present the aggregation using the three most effective rankers. For the third approach, we select the pair of rankers  $R_x$  and  $R_y$  that maximizes the selection measure  $M(R_x, R_y)$  expressed in Equation 6:

$$M(R_x, R_y) = \frac{1 + ef_{R_x} \times ef_{R_y}}{1 + cor(R_x, R_y)} \quad (6)$$

where  $ef_{R_x}$  denotes the effectiveness value for the ranker  $R_x$ , regardless the evaluation metric used (NDCG@10 or N-S Score), and  $cor(R_x, R_y)$  is the correlation between  $R_x$  and  $R_y$ . This is a modified measure adapted from the one proposed in (Valem and Pedronette, 2017).

Let  $\tau_A$  and  $\tau_B$  be two ranks, and  $n$  be the size of these ranks. The correlation between two rankers is given by the mean correlation of their ranks with respect to each query. We adopt Jaccard’s correlation, given by Equation 7. Other metrics were considered, but Jaccard was the one that achieved ranker combinations for rank aggregation with the best results, in preliminary analysis that we performed, considering the possibilities for computing  $cor(R_x, R_y)$  from Equation 6 as with Jaccard, Kendall Tau or Spearman. An equivalent

---

<sup>2</sup>For Ohsumed dataset, we implemented the rankers and extracted the ranks ourselves. For the other datasets, we adopted ranks built from previous works of our research group, namely (Pedronette et al., 2017; Pedronette and Torres, 2016), etc.

conclusion was observed in (Valem and Pedronette, 2017), that investigated possibilities for ranker selection.

Kendall Tau relies on the number of discordant pairs between  $\tau_A$  and  $\tau_B$ . Given two response items  $(s_i, s_j)$ , this pair is named discordant for  $\tau_A$  and  $\tau_B$  if  $\rho_{\tau_A}(s_i) > \rho_{\tau_B}(s_j)$  and  $\rho_{\tau_A}(s_j) > \rho_{\tau_B}(s_i)$ . Kendall Tau’s correlation is given by Equation 8, where  $K_d$  is the number of discordant pairs and  $n_d = \frac{n \times (n-1)}{2}$ . Spearman correlation relies on the position disparity of each response item in the two ranks, and it is given by Equation 9.

$$J(\tau_A, \tau_B) = \frac{|\tau_A \cap \tau_B|}{|\tau_A \cup \tau_B|} \quad (7)$$

$$K_s(\tau_A, \tau_B) = 1 - \frac{K_d(\tau_A, \tau_B)}{n_d} \quad (8)$$

$$S(\tau_A, \tau_B) = 1 - \frac{\sum_{s_i \in \tau_A} |\rho_{\tau_A}(s_i) - \rho_{\tau_B}(s_i)|}{n \times (n+1)} \quad (9)$$

Several state-of-the-art rank aggregation baselines are tested, along with our method, for the same candidate set of rankers: QueryRankFusion (Zhang et al., 2015), RecKNNGraphCCs (Pedronette et al., 2017), RkGraph (Pedronette et al., 2016), CorGraph (Pedronette and Torres, 2016), MRA, RRF, BordaCount, CombSUM, CombMIN, CombMAX, CombMED, CombANZ, CombMNZ, Condorcet, Kemeny, and RLSim. For UKBench, we also compare the results with the ones associated with the methods described in the following recent works: Bai and Bai (2016), Xie et al. (2015), Zheng et al. (2015), Zheng et al. (2014), Wang et al. (2012), and Qin et al. (2011).

We conduct statistical tests, using per-query paired t-test at 99% confidence level. We denote the statistical analysis with the following symbols:  $\blacktriangle$  indicates that our method was statistically better than the baseline,  $\blacktriangledown$  means the opposite, and  $\bullet$  means a statistical tie.

As we analyze a large number of datasets, fusion configurations (which rankers to fuse) and baselines, besides the statistical comparisons we also present the *winning number* (Tax et al., 2015) of each rank aggregation function, aiming

at providing a global performance indicator per method. The winning number of a method  $m$ ,  $W_m$ , regarding a performance measure  $P$ , is adapted to our context as in Equation 10, where  $D$  is the set of datasets,  $C_d$  is the set of our 3 pre-defined configurations for dataset  $d$  with respect to which rankers to fuse,  $P_m(d, c)$  is the performance of the method  $m$  on dataset  $d$  and configuration  $c \in C_d$ ,  $M$  is set of rank aggregation methods, and  $\mathbf{1}_{P_m(d) > P_k(d)}$  is the indicator function given by Equation 11.

$$W_m = \sum_{d \in D} \sum_{c \in C_d} \sum_{i \in M} \mathbf{1}_{P_m(d, c) > P_i(d, c)} \quad (10)$$

$$\mathbf{1}_{P_m(d, c) > P_i(d, c)} = \begin{cases} 1 & \text{if } P_m(d, c) > P_i(d, c), \\ 0 & \text{otherwise.} \end{cases} \quad (11)$$

### 5.3. Ranker Effectiveness and Correlations

Tables 4a, 4b, 4c, 4d, 4e, and 4f report the results obtained by the individual rankers, respectively for the datasets Brodatz, UW, MPEG-7, Ohsumed, UK-Bench, and Soccer. The rankers are presented sorted by their results. It can be noticed large variability in rankers' results. Furthermore, rankers perform differently depending on the dataset, possibly providing complementary views. For example, JACCARD was better than COSINE in UW, but the opposite happened for the Ohsumed dataset.

Tables 5, 6, 7, 8, 9, and 10 report the Jaccard's correlations between ranks for the individual rankers used, respectively for the datasets Brodatz, UW, MPEG-7, Ohsumed, UKBench, and Soccer. These correlations, along with the individual rankers' effectiveness, provide useful insights with respect to which rankers should be combined. In Ohsumed, WMD shows very low correlation to the other rankers, even though it was the worst effective ranker.

### 5.4. Rank Aggregation Results

We report the rank aggregation results obtained by our method and by the baselines, for each dataset and each of the three combinations of rankers. From

the evaluation procedure previously presented, the following combinations of rankers were selected per dataset:

- Brodatz: all 3 rankers; LAS + CCOM; LAS + LBP.
- Soccer: all 3; BIC + ACC; BIC + GCH.
- MPEG-7: all 6; ASC + AIR; AIR + CFD.
- Ohsumed: all 7; BoW-cosine + 2grams-cosine; BoW-cosine + WMD.
- UKBench: all 7; VOC + ACC; VOC + ACC + CNN-Caffe.
- UW: all 12; JAC + BIC; JAC + OKAPI.

Recall that the use of LAS + LBP and BIC + GCH for the Brodatz and the Soccer datasets, respectively, were defined according to Equation 6. The same approach was used for the other datasets. For UKBench, both second and third selection approaches lead to the same pair of rankers, so we also present the aggregation using its three most effective rankers.

Tables 11, 12, 13, 14, 15, and 16 report the results obtained, respectively for Ohsumed, Brodatz, MPEG-7, Soccer, UW, and UKBench.

Most baselines presented results worse than the best individual rankers, but our method overcame the individual rankers in all scenarios. It can be seen that most baselines are dramatically affected by bad individual ranks, in the sense that the addition of a poor ranker into the aggregation function leads to poor effectiveness. This may be seen as a negative aspect of unsupervised rank aggregation functions in general. Our method, on the contrary, was shown to be much less sensitive to this search scenario. For the Ohsumed dataset, for example, WMD performed much worse than BoW-cosine, but, because they produce low correlated ranks, their fusion still yielded a better ranker.

The criteria adopted to choose pairs of rankers for combination, based on effectiveness and correlation, led to pairs whose aggregated results surpassed pairs formed by the most effective rankers for the MPEG-7 and UW datasets.

Table 11: Results for rank aggregation on Ohsumed.

Method	NDCG@10			
	BoW-cosine + BoW-Jaccard + 2grams-cosine + 2grams-Jaccard + GNF-MCS + GNF-WGU + WMD	BoW- cosine + 2grams- cosine	BoW- cosine + WMD	
<b>FG</b>	0.683835	0.683472	0.676760	
RecKNNGraphCCs	▲ 0.676234	▲ 0.679728	▲ 0.667750	
CombSUM	▲ 0.666997	▲ 0.671868	▲ 0.598441	
CombMED	▲ 0.666997	▲ 0.671868	▲ 0.598441	
CombMNZ	▲ 0.666929	▲ 0.671869	▲ 0.598261	
QueryRankFusion	▲ 0.651279	▲ 0.671258	▲ 0.669704	
MRA	▲ 0.666045	▲ 0.670357	▲ 0.582049	
RRF	▲ 0.665793	▲ 0.671294	▲ 0.571016	
BordaCount	▲ 0.660197	▲ 0.671147	▲ 0.570466	
Condorcet	▲ 0.619869	▲ 0.670235	▲ 0.569906	
CombMAX	▲ 0.611777	▲ 0.671305	▲ 0.597080	
CombANZ	▲ 0.567671	▲ 0.670550	▲ 0.595983	
Kemeny	▲ 0.543564	▲ 0.665817	▲ 0.526588	
CombMIN	▲ 0.502482	▲ 0.666559	▲ 0.591361	
RLSim	▲ 0.434614	▲ 0.639004	▲ 0.579972	
CorGraph	▲ 0.487177	▲ 0.497431	▲ 0.456434	
RkGraph	▲ 0.289045	▼ 0.688443	▲ 0.288436	

Table 12: Results for rank aggregation on Brodatz.

Method	NDCG@10		
	LAS+CCOM+LBP	LAS+CCOM	LAS+LBP
RecKNNGraphCCs	● 0.877882	▼ 0.882903	▼ 0.839717
<b>FG</b>	0.878995	0.872084	0.835624
RkGraph	▲ 0.812659	▲ 0.861250	▲ 0.788682
QueryRankFusion	▲ 0.850263	▲ 0.850438	▲ 0.808562
CombMNZ	▲ 0.822887	▲ 0.827517	▲ 0.787922
CombSUM	▲ 0.812971	▲ 0.826075	▲ 0.784971
CombMED	▲ 0.812971	▲ 0.826075	▲ 0.784971
CombMAX	▲ 0.787828	▲ 0.818125	▲ 0.776842
RRF	▲ 0.818656	▲ 0.817139	▲ 0.788840
BordaCount	▲ 0.805699	▲ 0.814664	▲ 0.785836
MRA	▲ 0.822778	▲ 0.813396	▲ 0.788883
CombANZ	▲ 0.763987	▲ 0.812431	▲ 0.769743
Condorcet	▲ 0.781129	▲ 0.809929	▲ 0.781781
CorGraph	▲ 0.749420	▼ 0.895623	▲ 0.719204
CombMIN	▲ 0.713228	▲ 0.794631	▲ 0.752268
Kemeny	▲ 0.719680	▲ 0.786537	▲ 0.757349
RLSim	▲ 0.633157	▲ 0.756053	▲ 0.724879

Table 13: Results for rank aggregation on MPEG-7.

Method	NDCG@10		
	AIR + CFD + ASC + IDSC + BAS + SS	ASC + AIR	AIR + CFD
<b>FG</b>	0.997658	0.994729	0.995886
RecKNNGraphCCs	● 0.998052	● 0.995160	● 0.997267
RkGraph	▲ 0.826119	▼ 0.999350	▲ 0.992078
CorGraph	▲ 0.992456	▲ 0.962951	▲ 0.961460
RRF	▲ 0.980638	▲ 0.957684	▲ 0.954499
MRA	▲ 0.980086	▲ 0.950442	▲ 0.946144
CombMNZ	▲ 0.976832	▲ 0.942705	▲ 0.932234
BordaCount	▲ 0.974697	▲ 0.954296	▲ 0.951316
CombSUM	▲ 0.969212	▲ 0.941585	▲ 0.930685
CombMED	▲ 0.969212	▲ 0.941585	▲ 0.930685
QueryRankFusion	▲ 0.940976	▲ 0.941762	▲ 0.941271
CombMAX	▲ 0.930012	▲ 0.941585	▲ 0.930685
Condorcet	▲ 0.911624	▲ 0.950122	▲ 0.947416
CombANZ	▲ 0.862366	▲ 0.938649	▲ 0.927035
Kemeny	▲ 0.792694	▲ 0.940479	▲ 0.929906
CombMIN	▲ 0.626645	▲ 0.902798	▲ 0.888723
RLSim	▲ 0.444817	▲ 0.902798	▲ 0.888723



Table 14: Results for rank aggregation on Soccer.

Method	NDCG@10		
	BIC+ACC+GCH	BIC+ACC	BIC+GCH
<b>FG</b>	0.651828	0.655332	0.622217
RkGraph	● 0.653623	● 0.656422	● 0.628563
CorGraph	▲ 0.645004	▲ 0.643505	● 0.623627
RecKNNGraphCCs	▲ 0.637537	▲ 0.640729	● 0.618704
QueryRankFusion	▲ 0.613732	▲ 0.613659	▲ 0.598862
BordaCount	▲ 0.603156	▲ 0.613205	▲ 0.589633
RRF	▲ 0.604119	▲ 0.613005	▲ 0.590819
CombSUM	▲ 0.604575	▲ 0.611546	▲ 0.588667
CombMED	▲ 0.604565	▲ 0.611546	▲ 0.588667
CombMNZ	▲ 0.605567	▲ 0.611269	▲ 0.589202
MRA	▲ 0.605971	▲ 0.611017	▲ 0.588399
CombANZ	▲ 0.587048	▲ 0.610981	▲ 0.582010
Condorcet	▲ 0.593809	▲ 0.611049	▲ 0.589266
CombMAX	▲ 0.591911	▲ 0.609345	▲ 0.584983
Kemeny	▲ 0.578919	▲ 0.607451	▲ 0.578043
CombMIN	▲ 0.570258	▲ 0.606144	▲ 0.576877
RLSim	▲ 0.506736	▲ 0.570744	▲ 0.545591

Table 15: Results for rank aggregation on UW.

Method	NDCG@10		
	JAC + BIC + DICE + BOW + OKAPI + JACCARD + TF-IDF + GCH + COSINE + LAS + HTD + QCCH	JAC + BIC	JAC + OKAPI
CorGraph	▼ 0.896341	▲ 0.842665	▼ 0.933452
<b>FG</b>	0.873607	0.854473	0.882776
RecKNNGraphCCs	▲ 0.869448	▲ 0.843423	● 0.882035
RkGraph	▲ 0.746804	▲ 0.841127	▲ 0.866544
MRA	▲ 0.815983	▲ 0.797292	▲ 0.786995
RRF	▲ 0.815779	▲ 0.798502	▲ 0.795143
CombMNZ	▲ 0.806416	▲ 0.793488	▲ 0.814850
BordaCount	▲ 0.789620	▲ 0.797677	▲ 0.788127
CombSUM	▲ 0.769227	▲ 0.793057	▲ 0.812383
CombMED	▲ 0.769227	▲ 0.793057	▲ 0.812383
QueryRankFusion	▲ 0.747281	▲ 0.792681	▲ 0.807250
Condorcet	▲ 0.743168	▲ 0.795304	▲ 0.780080
CombMAX	▲ 0.691427	▲ 0.786912	▲ 0.802788
CombANZ	▲ 0.596119	▲ 0.784183	▲ 0.795284
Kemeny	▲ 0.471099	▲ 0.773449	▲ 0.739709
CombMIN	▲ 0.359668	▲ 0.773776	▲ 0.769389
RLSim	▲ 0.330593	▲ 0.740222	▲ 0.768275

Table 16: Results for rank aggregation on UKBench.

Method	N-S Score		
	VOC + ACC + CNN-Caffe + SCD + JCD + FCTH-SPy + CEDD-SPy	VOC + ACC	VOC + ACC + CNN-Caffe
<b>FG</b>	3.69	3.83	3.90
RecKNNGraphCCs	▲ 3.67	▲ 3.81	▲ 3.87
QueryRankFusion	▲ 3.60	▲ 3.78	▲ 3.86
MRA	▲ 3.52	▲ 3.50	▲ 3.77
CombSUM	▲ 3.55	▲ 3.60	▲ 3.76
CombMED	▲ 3.55	▲ 3.60	▲ 3.76
CombMNZ	▲ 3.53	▲ 3.60	▲ 3.76
BordaCount	▲ 3.55	▲ 3.60	▲ 3.76
RRF	▲ 3.52	▲ 3.60	▲ 3.76
Condorcet	▲ 3.64	▲ 3.58	▲ 3.75
CombMAX	▲ 3.13	▲ 3.52	▲ 3.48
RkGraph	▲ 3.03	▲ 3.50	▲ 3.54
CombANZ	▲ 2.83	▲ 3.42	▲ 3.28
Kemeny	▲ 2.51	▲ 3.37	▲ 3.14
CombMIN	▲ 2.35	▲ 3.36	▲ 3.09
CorGraph	▲ 2.44	▲ 2.91	▲ 2.77
RLSim	▲ 1.09	▲ 2.73	▲ 1.89

In most cases, the selection of the most effective base rankers yields suitable results.

In Ohsumed, Brodatz, and MPEG-7, the aggregation of all rankers performed better than the combination of selected pairs of rankers. These results demonstrate that even less competitive rankers can contribute to improving retrieval tasks when used in the aggregation.

While the ranker selection criteria of using all rankers led to top performance in half the datasets, it also demands additional processing cost. The analysis of the three ranker selection approaches given allows us to conclude that the ranker selection of the two most competitive rankers per dataset is an overall good choice, but subject to improvement after a careful empirical evaluation of the other approaches in the desired scenario.

We summarize in Table 17 the results achieved by the rankers in each dataset, and report our gains over them, in percentage gain. *FG* was able to present significant gains over the rankers.

Our method achieved either top or very competitive performance in all datasets and combinations of rankers tested. For 6 datasets with 3 configurations each, and for 16 state-of-the-art baselines, *FG* was statistically worse only in 7 out of 288 comparisons. Besides, it was top-1 in 4 out of 6 datasets (Ohsumed, MPEG-7, Soccer, and UKBench), and top-2 in Brodatz and UW.

We present in Figure 4 the winning numbers achieved per rank aggregation function, in order to contrast them globally. *FG* was broadly superior to the majority of baselines, according to our experimental evaluation comprising 3 aggregation approaches for each of the 6 distinct datasets used.

Table 18 presents the results of our ranker for UKBench, together with seven additional baselines. The table reports the results from Table 16, obtained using ACC + VOC + CNN-Caffe, together with results reported by the other baselines. QueryRankFusion is presented twice, one regarding their own reported result, and another considering the same input rankers as ours. It is worth to notice that three of these additional baselines performed worse than some classic and much simpler rank aggregation functions. Again, our method achieved the

Table 17: Effectiveness of rankers compared to our method, in textual, image, and hybrid datasets.

(a) Brodatz			(c) MPEG-7			(e) UKBench		
Method	NDCG@10	Gains (%)	Method	NDCG@10	Gains (%)	Method	N-S Score	Gains (%)
<b>FG</b>	0.878995		<b>FG</b>	0.997658		<b>FG</b>	3.90	
LAS	0.850533	3.35	ASC	0.941585	5.96	VOC	3.54	10.17
CCOM	0.726186	21.04	AIR	0.939424	6.20	ACC	3.37	15.73
LBP	0.652759	33.66	CFD	0.930685	7.20	CNN-Caffe	3.31	17.83
(b) UW dataset			IDSC	0.922828	8.11	SCD	3.15	23.81
			BAS	0.866098	15.19	JCD	2.79	39.79
			SS	0.611481	63.15	FCTH-SPy	2.73	42.86
						CEDD-SPy	2.61	49.43
Method	NDCG@10	Gains (%)	(d) Ohsumed			(f) Soccer		
<b>FG</b>	0.873607		Method	NDCG@10	Gains (%)	Method	NDCG@10	Gains (%)
JAC	0.810729	7.76	<b>FG</b>	0.683835		<b>FG</b>	0.655332	
BIC	0.746454	17.03	BoW-cosine	0.669701	2.11	BIC	0.614818	6.59
DICE	0.722831	20.86	2grams-cosine	0.664120	2.97	ACC	0.592699	10.57
BOW	0.720781	21.20	GNF-WGU	0.662668	3.19	GCH	0.536412	22.17
OKAPI	0.716035	22.01	GNF-MCS	0.655420	4.34			
JACCARD	0.701651	24.51	2grams-Jaccard	0.651320	4.99			
TF-IDF	0.658880	32.59	BoW-Jaccard	0.645711	5.90			
GCH	0.630315	38.60	WMD	0.427361	60.01			
COSINE	0.554767	57.47						
LAS	0.514314	69.86						
HTD	0.495002	76.49						
QCCH	0.414249	110.89						

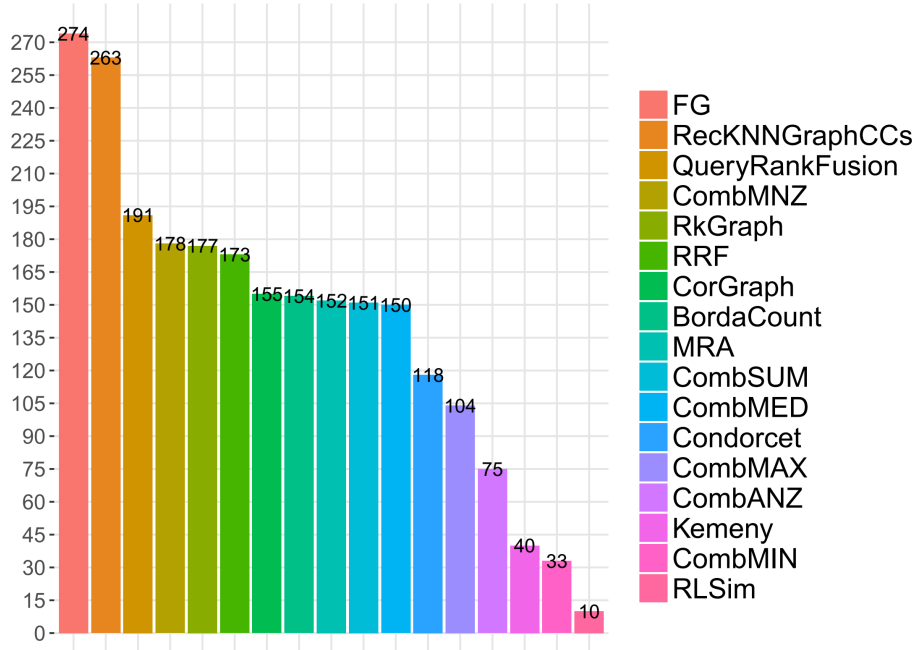


Figure 4: Winning numbers achieved per rank aggregation function.

best performance.

Our rank fusion has been shown to be effective in combining contextual information from different ranks, along with the intrinsic relationships that the retrieved objects have to each other in their own ranks. Also, our procedure to rank objects based on fusion graphs considers these fusions automatically, relying on such graphs without any other intermediate steps, such as training or parameter tuning.

### 5.5. Efficiency Analysis

Section 4.3 presents the computational cost analysis of our method. The time for performing a query is around the sum of the slowest time to produce an isolated rank plus the time to produce the final rank based on fusion graphs. Table 19 presents, per dataset, the mean time (in milliseconds) spent per query. We report the mean time of 5 independent measurements, taken on an Intel Core i7-7500U CPU @ 2.70GHz with 16GB of RAM. For all datasets, the search times

Table 18: State-of-the-art results on UKBench. Results marked with \* were obtained using ACC + VOC + CNN-Caffe.

Method	N-S Score
<b>FG</b>	<b>3.90*</b>
Xie et al. (2015)	3.89
RecKNNGraphCCs	3.87*
Bai and Bai (2016)	3.86
QueryRankFusion	3.86*
Zheng et al. (2015)	3.84
QueryRankFusion	3.83
MRA	3.77*
CombSUM	3.76*
CombMED	3.76*
CombMNZ	3.76*
BordaCount	3.76*
RRF	3.76*
Condorcet	3.75*
Wang et al. (2012)	3.68
Qin et al. (2011)	3.67
Zheng et al. (2014)	3.57
RkGraph	3.54*
CombMAX	3.48*
CombANZ	3.28*
Kemeny	3.14*
CombMIN	3.09*
CorGraph	2.91*
RLSim	1.89*

were reasonable, given the high gains in effectiveness provided by our method.

Table 19: Mean rank aggregation time per query per dataset.

Dataset	Time (in ms)
Brodatz	$8.76 \pm 2.70$
MPEG-7	$25.73 \pm 2.76$
Ohsumed	$101.13 \pm 16.88$
Soccer	$4.60 \pm 2.58$
UW	$29.29 \pm 7.80$
UKBench	$21.30 \pm 6.68$

## 6. Conclusions

Distinct features provide different and complementary views of textual and multimedia documents in retrieval tasks. Therefore, combining such results for a more effective retrieval without the need of user intervention remains a relevant and challenging task.

In this paper, a novel unsupervised graph-based rank aggregation method is proposed. Our approach models the rank fusion task by means of a fusion graph and derives a novel fused retrieval score, directly based on the graph structure. The method was extensively evaluated on textual, images, and hybrid datasets comprising ad-hoc retrieval tasks, achieving superior effectiveness scores than the best isolated features and several baselines.

As a future work, we intend to evaluate our method against supervised techniques. We also want to explore other rank-fusion vector representations based on graphs. The goal is to take advantages of existing solutions (e.g., indexing schemes) to make our fusion method even more scalable.



## References

## References

- Arica, N., Vural, F.T.Y., 2003. Bas: a perceptual shape descriptor based on the beam angle statistics. *Pattern Recognition Letters* 24, 1627–1639. doi:doi:10.1016/s0167-8655(03)00002-3.
- Baeza-Yates, R., Ribeiro-Neto, B., 1999. *Modern information retrieval*. Addison-Wesley, Boston, MA, USA.
- Bai, S., Bai, X., 2016. Sparse contextual activation for efficient visual re-ranking. *IEEE Transactions on Image Processing* 25, 1056–1069. doi:doi:10.1109/tip.2016.2514498.
- Borda, J.C., 1784. *Mémoire sur les élections au scrutin*. Histoire de l’Academie Royale des Sciences pour 1781 (Paris, 1784) .
- Brodatz, P., 1966. *Textures: A photographic album for artists and designers*. Dover. doi:doi:10.2307/1571915.
- Bunke, H., Shearer, K., 1998. A graph distance metric based on the maximal common subgraph. *Pattern Recognition Letters* 19, 255–259. doi:doi:10.1016/s0167-8655(97)00179-7.
- Carrillo, M., Villatoro-Tello, E., López-López, A., Eliasmith, C., Montes-y Gómez, M., Pineda, L.V., 2009. Representing context information for document retrieval, in: *8th FQAS’09*, Springer, Berlin, Heidelberg. pp. 239–250. doi:doi:10.1007/978-3-642-04957-6\_21.
- Chatzichristofis, S.A., Boutalis, Y.S., 2008a. Cedd: Color and edge directivity descriptor: A compact descriptor for image indexing and retrieval, in: *International Conference on Computer Vision Systems*, Springer. pp. 312–322. doi:doi:10.1007/978-3-540-79547-6\_30.

- Chatzichristofis, S.A., Boutalis, Y.S., 2008b. Fcth: Fuzzy color and texture histogram - a low level feature for accurate image retrieval, in: WIAMIS'08, IEEE. pp. 191–196. doi:doi:10.1109/WIAMIS.2008.24.
- Cormack, G.V., Clarke, C.L.A., Buettcher, S., 2009. Reciprocal rank fusion outperforms condorcet and individual rank learning methods, in: Proc. ACM SIGIR, ACM. pp. 758–759. doi:doi:10.1145/1571941.1572114.
- Deselaers, T., Keysers, D., Ney, H., 2008. Features for image retrieval: an experimental comparison. *Information Retrieval* 11, 77–107. doi:doi:10.1007/s10791-007-9039-3.
- Dickinson, P.J., Bunke, H., Dadej, A., Kraetzel, M., 2004. Matching graphs with unique node labels. *Pattern Analysis and Applications* 7, 243–254. doi:doi:10.1007/s10044-004-0222-5.
- Dwork, C., Kumar, R., Naor, M., Sivakumar, D., 2001. Rank aggregation methods for the web, in: 10th WWW'01, ACM, New York, NY, USA. pp. 613–622. doi:doi:10.1145/371920.372165.
- Fagin, R., Kumar, R., Sivakumar, D., 2003. Efficient similarity search and classification via rank aggregation, in: Proceedings of the 2003 ACM SIGMOD international conference on Management of data, ACM. pp. 301–312. doi:doi:10.1145/872757.872795.
- Fox, E.A., Shaw, J.A., 1994. Combination of multiple searches, in: Proc. 2nd Text REtrieval Conference (TREC-2), pp. 243–252.
- Gopalan, R., Turaga, P., Chellappa, R., 2010. Articulation-invariant representation of non-planar shapes, in: Proceedings of the 11th European Conference on Computer Vision, Springer, Berlin, Heidelberg. pp. 286–299. doi:doi:10.1007/978-3-642-15558-1\_21.
- Hersh, W., Buckley, C., Leone, T.J., Hickam, D., 1994. Ohsumed: an interactive retrieval evaluation and new large test collection for research, in: SIGIR'94, Springer. pp. 192–201. doi:doi:10.1007/978-1-4471-2099-5\_20.

- Huang, C.B., Liu, Q., 2007. An orientation independent texture descriptor for image retrieval, in: ICCCAS'07, pp. 772–776. doi:doi:10.1109/ICCCAS.2007.4348164.
- Huang, J., Kumar, S.R., Mitra, M., Zhu, W.J., Zabih, R., 1997. Image indexing using color correlograms, in: Proc. IEEE CVPR'97, IEEE. pp. 762–768. doi:doi:10.1109/CVPR.1997.609412.
- Hubert, G., Pitarch, Y., Pinel-Sauvagnat, K., Tournier, R., Laporte, L., 2018. Tournarank: When retrieval becomes document competition. *Information Processing & Management* 54, 252 – 272. doi:doi:10.1016/j.ipm.2017.11.006.
- Jegou, H., Schmid, C., Harzallah, H., Verbeek, J., 2010. Accurate image search using the contextual dissimilarity measure. *IEEE Transactions on Pattern Analysis and Machine Intelligence* 32, 2–11. doi:doi:10.1109/TPAMI.2008.285.
- Jia, Y., Shelhamer, E., Donahue, J., Karayev, S., Long, J., Girshick, R., Guadarrama, S., Darrell, T., 2014. Caffe: Convolutional architecture for fast feature embedding, in: Proc. 22Nd ACM MM'14, ACM, New York, NY, USA. pp. 675–678. doi:doi:10.1145/2647868.2654889.
- Kaur, P., Singh, M., Singh Josan, G., 2017. Comparative analysis of rank aggregation techniques for metasearch using genetic algorithm. *Education and Information Technologies* 22, 965–983. doi:doi:10.1007/s10639-016-9467-z.
- Kovalev, V., Volmer, S., 1998. Color co-occurrence descriptors for querying-by-example, in: *Multimedia Modeling*, IEEE. pp. 32–38. doi:doi:10.1109/mulmm.1998.722972.
- Kusner, M., Sun, Y., Kolkin, N., Weinberger, K., 2015. From word embeddings to document distances, in: *International Conference on Machine Learning*, pp. 957–966.
- Latecki, L.J., Lakamper, R., Eckhardt, T., 2000. Shape descriptors for non-rigid shapes with a single closed contour, in: *Computer Vision and Pattern*

- Recognition, 2000. Proceedings. IEEE Conference on, IEEE. pp. 424–429. doi:doi:10.1109/cvpr.2000.855850.
- Lewis, J., Ossowski, S., Hicks, J., Errami, M., Garner, H.R., 2006. Text similarity: an alternative way to search medline. *Bioinformatics* 22, 2298–304. doi:doi:10.1093/bioinformatics/btl388.
- Ling, H., Jacobs, D.W., 2007. Shape classification using the inner-distance. *IEEE Transactions on Pattern Analysis and Machine Intelligence* 29, 286–299. doi:doi:10.1109/tpami.2007.41.
- Ling, H., Yang, X., Latecki, L.J., 2010. Balancing deformability and discriminability for shape matching, in: *ECCV*, Springer. pp. 411–424. doi:doi:10.1007/978-3-642-15558-1\_30.
- Lux, M., 2011. Content based image retrieval with lire, in: *Proc. 19th ACM MM’11*, ACM, New York, NY, USA. pp. 735–738. doi:doi:10.1145/2072298.2072432.
- Manjunath, B.S., Ohm, J.R., Vasudevan, V.V., Yamada, A., 2001. Color and texture descriptors. *IEEE Transactions on circuits and systems for video technology* 11, 703–715. doi:doi:10.1109/76.927424.
- Mikolov, T., Sutskever, I., Chen, K., Corrado, G., Dean, J., 2013. Distributed representations of words and phrases and their compositionality, in: *Proc. NIPS’13*, pp. 3111–3119.
- Mourão, A., Magalhães, J., 2018. Low-complexity supervised rank fusion models, in: *Proceedings of the 27th ACM International Conference on Information and Knowledge Management*, ACM, New York, NY, USA. pp. 1691–1694. doi:doi:10.1145/3269206.3269316.
- Nistér, D., Stewenius, H., 2006. Scalable recognition with a vocabulary tree, in: *IEEE Computer Society Conference on Computer Vision and Pattern Recognition*, IEEE. pp. 2161–2168. doi:doi:10.1109/cvpr.2006.264.

- Ojala, T., Pietikainen, M., Maenpaa, T., 2002. Multiresolution gray-scale and rotation invariant texture classification with local binary patterns. *IEEE Transactions on Pattern Analysis and Machine Intelligence* 24, 971–987. doi:doi:10.1109/tpami.2002.1017623.
- Pedronette, D.C.G., Almeida, J., Torres, R.d.S., 2016. A graph-based ranked-list model for unsupervised distance learning on shape retrieval. *Pattern Recognition Letters* 83, 357–367.
- Pedronette, D.C.G., Gonçalves, F.M.F., Guilherme, I.R., 2017. Unsupervised manifold learning through reciprocal knn graph and connected components for image retrieval tasks. *Pattern Recognition* 75, 161 – 174. doi:doi:10.1016/j.patcog.2017.05.009.
- Pedronette, D.C.G., Torres, R.d.S., 2010. Shape retrieval using contour features and distance optimization, in: *Proceedings of the International Conference on Computer Vision Theory and Applications*, pp. 197–202. doi:doi:10.5220/0002837201970202.
- Pedronette, D.C.G., Torres, R.d.S., 2013. Image re-ranking and rank aggregation based on similarity of ranked lists. *Pattern Recognition* 46, 2350–2360. doi:doi:10.1016/j.patcog.2013.01.004.
- Pedronette, D.C.G., Torres, R.d.S., 2016. A correlation graph approach for unsupervised manifold learning in image retrieval tasks. *Neurocomputing* 208, 66–79.
- Qin, D., Gammeter, S., Bossard, L., Quack, T., van Gool, L., 2011. Hello neighbor: Accurate object retrieval with k-reciprocal nearest neighbors, in: *IEEE CVPR’11, IEEE*. pp. 777–784. doi:doi:10.1109/cvpr.2011.5995373.
- Robertson, S.E., Walker, S., Jones, S., Hancock-Beaulieu, M., Gatford, M., 1994. Okapi at trec-3, in: *Text REtrieval Conference*, pp. 109–126.
- Schenker, A., Bunke, H., Last, M., Kandel, A., 2007. Clustering of web documents using graph representations, in: *Applied Graph Theory in Com-*

- puter Vision and Pattern Recognition. Springer, pp. 247–265. doi:doi:10.1007/978-3-540-68020-8\_10.
- Sculley, D., 2007. Rank aggregation for similar items, in: SIAM International Conference on Data Mining, pp. 587–592. doi:doi:10.1137/1.9781611972771.66.
- Silva, F.B., Werneck, R.O., Goldenstein, S., Tabbone, S., Torres, R.S., 2018. Graph-based bag-of-words for classification. *Pattern Recognition* 74, 266 – 285. doi:doi:10.1016/j.patcog.2017.09.018.
- Stehling, R.O., Nascimento, M.A., Falcão, A.X., 2002. A compact and efficient image retrieval approach based on border/interior pixel classification, in: Proceedings of the eleventh International Conference on Information and Knowledge Management, ACM. pp. 102–109. doi:doi:10.1145/584792.584812.
- Swain, M.J., Ballard, D.H., 1991. Color indexing. *International journal of computer vision* 7, 11–32. doi:doi:10.1007/BF00130487.
- Tao, B., Dickinson, B.W., 2000. Texture recognition and image retrieval using gradient indexing. *Journal of Visual Communication and Image Representation* 11, 327–342. doi:doi:10.1006/jvci.2000.0448.
- Tax, N., Bockting, S., Hiemstra, D., 2015. A cross-benchmark comparison of 87 learning to rank methods. *Information Processing & Management* 51, 757 – 772. doi:doi:10.1016/j.ipm.2015.07.002.
- Torres, R.d.S., Falcão, A.X., 2007. Contour salience descriptors for effective image retrieval and analysis. *Image and Vision Computing* 25, 3–13. doi:doi:10.1016/j.imavis.2005.12.010.
- Valem, L.P., Pedronette, D.C.G., 2017. Selection and combination of unsupervised learning methods for image retrieval, in: Proc. of the 15th International Workshop on Content-Based Multimedia Indexing, ACM. p. 27. doi:doi:10.1145/3095713.3095741.

- Van De Weijer, J., Schmid, C., 2006. Coloring local feature extraction. *Computer Vision–ECCV 2006*, 334–348doi:doi:10.1007/11744047\_26.
- Wallis, W.D., Shoubbridge, P., Kraetz, M., Ray, D., 2001. Graph distances using graph union. *Pattern Recognition Letters* 22, 701–704. doi:doi:10.1016/s0167-8655(01)00022-8.
- Wang, B., Jiang, J., Wang, W., Zhou, Z.H., Tu, Z., 2012. Unsupervised metric fusion by cross diffusion, in: *IEEE CVPR’12, IEEE*. pp. 2997–3004. doi:doi:10.1109/cvpr.2012.6248029.
- Wang, X., Yang, M., Cour, T., Zhu, S., Yu, K., Han, T.X., 2011. Contextual weighting for vocabulary tree based image retrieval, in: *2011 International Conference on Computer Vision, IEEE*. pp. 209–216. doi:doi:10.1109/ICCV.2011.6126244.
- Williams, A., Yoon, P., 2007. Content-based image retrieval using joint correlograms. *Multimedia Tools and Applications* 34, 239–248. doi:doi:10.1007/s11042-006-0087-2.
- Wu, P., Manjunanth, B.S., Newsam, S.D., Shin, H.D., 1999. A texture descriptor for image retrieval and browsing, in: *IEEE Workshop on Content-Based Access of Image and Video Libraries*, pp. 3–7.
- Xie, L., Hong, R., Zhang, B., Tian, Q., 2015. Image classification and retrieval are one, in: *Proc. 5th ACM ICMR’15, ACM, New York, NY, USA*. pp. 3–10. doi:doi:10.1145/2671188.2749289.
- Zagoris, K., Chatzichristofis, S.A., Papamarkos, N., Boutalis, Y.S., 2010. Automatic image annotation and retrieval using the joint composite descriptor, in: *2010 14th Panhellenic Conference on Informatics, IEEE*. pp. 143–147. doi:doi:10.1109/PCI.2010.38.
- Zhang, S., Yang, M., Cour, T., Yu, K., Metaxas, D.N., 2015. Query specific rank fusion for image retrieval. *IEEE Transactions on Pattern Analysis and Machine Intelligence* 37, 803–815. doi:doi:10.1109/tpami.2014.2346201.

- Zhao, W., Mao, J., Lu, K., 2018. Ranking themes on co-word networks: Exploring the relationships among different metrics. *Information Processing & Management* 54, 203 – 218. doi:doi:10.1016/j.ipm.2017.11.005.
- Zheng, L., Wang, S., Tian, L., He, F., Liu, Z., Tian, Q., 2015. Query-adaptive late fusion for image search and person re-identification, in: *Proc. IEEE CVPR'15, IEEE*. pp. 1741–1750. doi:doi:10.1109/cvpr.2015.7298783.
- Zheng, L., Wang, S., Tian, Q., 2014.  $\mathcal{L}_p$ -norm idf for scalable image retrieval. *IEEE Transactions on Image Processing* 23, 3604–3617. doi:doi:10.1109/tip.2014.2329182.
- Zhu, Y., Yu, J.X., Qin, L., 2014. Leveraging graph dimensions in online graph search. *Proc. VLDB'14* 8, 85–96. doi:doi:10.14778/2735461.2735469.